LOW EXCESS SPEED TRIPLE CYCLERS OF VENUS, EARTH, AND MARS

Drew Ryan Jones,* **Sonia Hernandez**,* **and Mark Jesick***

Ballistic cycler trajectories which repeatedly encounter Earth and Mars may be invaluable to a future transportation architecture ferrying humans to and from Mars. Such trajectories which also involve at least one flyby of Venus are computed here for the first time. The so-called triple cyclers are constructed to exhibit low excess speed on Earth-Mars and Mars-Earth transit legs, and thereby reduce the cost of hyperbolic rendezvous. Thousands of previously undocumented two synodic period Earth-Mars-Venus triple cyclers are discovered. Many solutions are identified with average transit leg excess speed below 5 km/sec, independent of encounter epoch. The energy characteristics are lower than previously documented cyclers not involving Venus, but the repeat periods are generally longer.

NOMENCLATURE

Δt_H	Earth-Mars Hohmann transfer flight time, days
δ	Hyperbolic flyby turning angle, degrees
$\hat{R},\ \hat{S},\ \hat{T}$	B-plane unit vectors
$\mathbf{B}$	B-plane vector, km
μ	Gravitational parameter, km^3/sec^2
θ_B	B-plane angle between $\mathbf{B}$ and $\hat{T}$, degrees
r_p	Periapsis radius, km
T	Cycler repeat period, days
t_0	Cycle starting epoch
t_0^*	Earth-Mars Hohmann transfer epoch
t_f	Cycle ending epoch
T_{syn}	Venus-Earth-Mars synodic period, days
v_∞	Hyperbolic excess speed, km/sec

INTRODUCTION

Trajectories are computed which ballistically and periodically cycle between flybys of Venus, Earth, and Mars. Using only gravity assists, a cycling vehicle returns to the starting body after a flight time commensurate with the celestial bodies' orbital periods, thereby permitting indefinite repetition. The repeatability and lack of propulsive maneuvers makes these trajectories attractive for mission applications in both human and robotic spaceflight. Cyclers involving just Earth and Mars have been studied extensively,[1–3] and these repeatable encounter orbits could play an important

---

*Mission Design and Navigation Section, Jet Propulsion Laboratory, California Institute of Technology, 4800 Oak Grove Drive, Pasadena, California 91109.

role in a future Mars colonization effort. For example, placing the large interplanetary transport on a cycler permits habitation, structure, and shielding to be reused, while small taxi vehicles can shuttle people and cargo to and from planets using much less fuel. Hence, rather than accelerating, decelerating, and possibly discarding the habitation module for each leg of an interplanetary flight, a cycler system enables reuse. Once the habitation is placed on the cycler trajectory, crew and cargo may be shuttled between planets using little fuel.[3] In this paper, the cycler is extended to three planets (so-called triple cycler) for the first time. Figure 1 illustrates a theoretical transportation architecture utilizing the triple cycler trajectory.
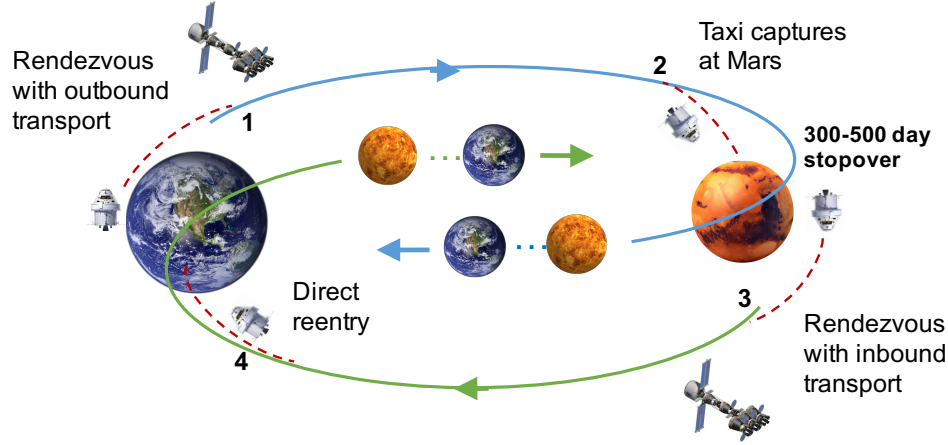
Figure 1: Earth-Mars transportation architecture using triple cycler trajectories

Background

Various authors have presented methods to compute and evaluate Earth-Mars cyclers.[1–4] Additionally, Landau and Longuski consider semi-cyclers as an alternative option for Mars exploration.[5] To the authors' knowledge, the literature contains only two references to triple cyclers,[6,7] and none which involve the planets. In a contemporaneous paper by Hernandez, Jones, and Jesick, the triple cycler concept and a similar search methodology are applied to the Jovian moon triplet Io-Europa-Ganymede.[8] The extension (to the moons) yields an alternative method for constructing a tour, and these cyclers are particularly exact due to the near perfect resonance of the moons.

Most analyzed families of Earth-Mars cyclers suffer from large maintenance maneuvers in the true ephemeris,[1] or high excess speed (v_∞) for certain opportunities.[1,2] Since landed spacecraft need to perform hyperbolic rendezvous with the cycling transport, low v_∞ is a very important performance metric. The addition of Venus as a flyby body may help maintain low v_∞ at Earth and Mars across transport opportunities. Previously it has been shown that adding a Venus flyby can improve the energy characteristics of trajectories encountering Earth and Mars,[9] and doing so can enable Earth-Mars free-return orbits.[10]

The search methodology developed here locates triple cycler trajectories which exhibit low transit leg v_∞ at Earth and Mars (near-Hohmann). Transit legs are those where people/cargo are aboard, and the remaining legs are used to setup the next periodic transit leg, via gravity assist flybys. We denote *outbound* cyclers as those cyclers with favorable Earth-Mars legs (low v_∞ within reasonable flight time), and *inbound* cyclers as those with favorable Mars-Earth legs.

Triple cycler families

The time it takes to repeat a given angular alignment of the three planets (the synodic period T_{syn}) is approximately 6.4 years. This is about three Earth-Mars synodic periods, and the three planets inertially align approximately every 32 years, or 5 T_{syn}. The following definitions are used throughout this work:

- **Cycle:** Portion of trajectory with flight time equal to an integer number of T_{syn}, and that starts and ends at the same body (Earth or Mars in this work).

- **Repeat period:** The flight time of a single cycle.

- **Cycler:** Trajectory that completes one or more cycles.

Cycler solutions are categorized into families based on the integer number of synodic periods in a cycle, and the itinerary of flybys (the order of bodies encountered). Additionally, the initialization year is important since that dictates the Earth-Mars (or Mars-Earth) opportunity. The opportunities open every 2.13 years. For this paper, attention is restricted to families with 1 or 2 synodic periods in a cycle, and a maximum of six flybys per cycle (this avoids extremely long repeat times). The desire to have low v_∞ transit legs, is explicitly enforced on the search method, which in turn limits the possible combinations. Specifically, each *outbound* cycler begins with a near-Hohmann Earth-to-Mars arc (Mars-to-Earth for *inbound*).

From an energy standpoint, a near-Hohmann Earth-to-Mars transfer cannot reach Venus in the next encounter, without re-encountering Earth. This is because the minimum energy transfer between Earth and Mars gives a v_∞ at Mars of 2-3 km/sec, whereas the minimum energy transfer between Mars and Venus gives v_∞ at Mars of around 5 km/sec. Similarly, a Venus flyby cannot immediately precede a near-Hohmann *inbound* Mars-to-Earth transit leg. These limitations are also apparent by examining a Tisserand plot or other energy-based (i.e. phase free) graphical tool.[11] With these constraints, the complete enumerated itineraries are limited to those in Table 1.

Table 1: Triple cycler itinerary combinations

Outbound	Inbound
EMEVE	MEVEM
EMEEVE	MEEVEM
EMEVVE	MEVVEM
EMEVEE	MEVEEM
EMMEVE	MEVEMM

To illustrate an itinerary family, consider the EMEEVE case. This begins with a near-Hohmann Earth to Mars transit leg (EM), followed by two Earth encounters (EE), a single Venus encounter (V), and finally returning to Earth (E) to complete a single cycle. The second cycle immediately follows with the next Earth to Mars transit. With the exception of the initial leg, the transfers between bodies may involve different flight times and number of revolutions. The number of T_{syn} to complete the encounters (EMEEVE) completely specifies a family.

Understanding the triple cycler

To qualitatively comprehend the triple cycler trajectory, and in particular the Venus flyby, the Tisserand graph or plot is useful.[11] These plots indicate possible gravity assist connections from an

energy-only perspective. By plotting contours in v_∞ for a given body over the full range of pump angle we can visualize how bodies may be connected and at what energy levels. A pump angle and v_∞ value map to semi-major axis and eccentricity and therefore to any related orbital parameters such as energy, periapsis radius, and apoapsis radius. Figure 2 presents a Tisserand graph generated using a simplified circular coplanar Solar System model for Venus, Earth, and Mars. This also highlights how a triple cycler trajectory could traverse the graph. Note that the contours for Mars (in red) do not intersect the Venus contours (in green) at these (relatively low) v_∞ levels, and hence a direct Mars-Venus transfer is not permitted. The tick marks indicate the maximum move along a contour with a single flyby (for a given v_∞, the maximum turning angle is limited by the radius of the planet).
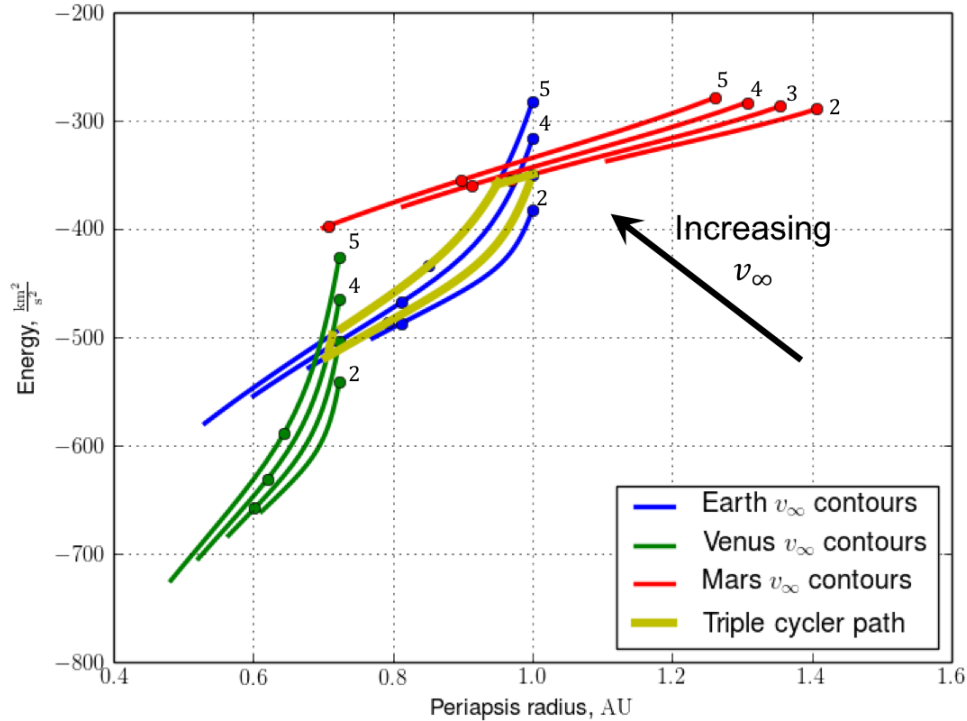
Figure 2: Venus-Earth-Mars Tisserand graph with v_∞ from 2 to 5 km/sec and v_∞ increasing from lower right to upper left

From the plot, a transfer can occur from Earth's 5 km/sec contour to Mars's 3 km/sec contour. A gravity assist from Mars increases the heliocentric energy and places the vehicle on Earth's 3 km/sec contour. From here it is generally not possible to reach Mars in the true ephemeris (especially considering Mars' eccentricity). A maneuver is generally necessary to place the vehicle back onto the higher energy contour for the next Earth-to-Mars opportunity. However, a move can be made downward (lower energy) along the contour using an Earth gravity assist to setup a Venus encounter along Venus's 4 km/sec contour. This returns the vehicle to the original Earth energy level in time for the next transit to Mars. This example represents a potentially low-energy *inbound* cycler.

In summary, Earth and Venus encounters are used between Earth-Mars (or Mars-Earth) transits to maintain the original low energy level which is disrupted by the encounter with Mars. Without the additional flybys, higher energy (and more costly) transfers must be accepted for some opportunities

or fairly large deep-space maneuvers must be used to move back to a low-energy contour. Such deficiencies occur in well-known Earth-Mars cyclers like the Aldrin[1] and S1L1.[2]

METHODOLOGY

A broad search algorithm is developed to identify near-ballistic cycler solutions using approximate dynamics. A zero-sphere-of-influence patched conic gravity model is used with the real planetary ephemeris, and Lambert's problem is solved to determine legs connecting consecutive encounters. Starting from the set of near-Hohmann transit legs, the remaining legs are evaluated by solving Lambert's problem over a discrete grid of flight times. Flight time is the primary search variable, but the revolutions from one to the maximum possible are considered, along with the fast/slow Lambert arc cases.* In general, Lambert's problem admits four solutions for a given number of revolutions, but here only prograde transfers are considered. Transfers which are an exact integer multiple of π are also not considered (Russell provides an excellent detailed summary of Lambert's problem and the possible solutions[12]). The Lambert arcs yield incoming and outgoing asymptotes at each encounter, and these are evaluated to be near-ballistic flybys with altitude between 100 km and 100,000 km.

Flyby Evaluation

After solving Lambert's problem for adjacent legs, powered hyperbolic flybys are computed. The flybys are necessary to evaluate constraints and remove solutions with infeasible altitude or where large velocity increments are necessary to correct the v_∞ discontinuity. Generally, velocity increments below 200 m/sec are permitted since experience has shown these can be differentially corrected in high-fidelity dynamics to be entirely ballistic.

Tangential periapsis maneuvers are calculated at each encounter to account for the v_∞ mismatch.[13] Such a maneuver is often sub-optimal; however, the guess suffices for filtering poor solutions via constraint evaluation. The transfer angle is:

$$\delta = \langle \mathbf{v}_\infty^-, \mathbf{v}_\infty^+ \rangle \tag{1}$$

The periapsis radius r_p is solved iteratively.†

$$\sin^{-1}\left(\frac{\mu}{\mu + r_p v_\infty^{-2}}\right) + \sin^{-1}\left(\frac{\mu}{\mu + r_p v_\infty^{+2}}\right) = \delta \tag{2}$$

With r_p known, the periapsis speeds before and after the impulse are:

$$v_p^- = \sqrt{v_\infty^{-2} + \frac{2\mu}{r_p}} \qquad v_p^+ = \sqrt{v_\infty^{+2} + \frac{2\mu}{r_p}} \tag{3}$$

Energy and eccentricity before and after the maneuver are readily derived. Since the maneuver is tangential, motion occurs in a plane containing the two asymptotes and the B-plane vector $\mathbf{B}$. The

---

*Fast/slow cases are also referred to as type 1 and type 2 in the literature.
†This allows subsurface solutions, but those are handled by a minimum altitude constraint.

two asymptotes fully define the plane (unless they are collinear). The orthogonal set of B-plane unit vectors, defined in a body-centered equatorial plane are:

$$\hat{S} = \frac{\mathbf{v}_\infty^-}{v_\infty^-} \qquad \hat{T} = \frac{(\mathbf{v}_\infty^-/v_\infty^-) \times \hat{k}}{\| (\mathbf{v}_\infty^-/v_\infty^-) \times \hat{k}\|} \qquad \hat{R} = \hat{S} \times \hat{T} \qquad (4)$$

Where $\hat{k}$ is the unit vector of the pole $(0, 0, 1)$.

The flyby bends the excess velocity vector such that the projection of $\mathbf{v}_\infty^+$ onto the B-plane is along the $-\mathbf{B}$ vector. Therefore, the angle of $\mathbf{B}$ relative to $\hat{T}$ is computed as:

$$\theta_B = \text{atan2}(\frac{\mathbf{v}_\infty^+}{v_\infty^+} \cdot \hat{R} , \ \frac{\mathbf{v}_\infty^+}{v_\infty^+} \cdot \hat{T}) - \pi \qquad (5)$$

Where atan2 is the quadrant specific arctan function with range $(\pi, -\pi]$. With θ_B, two periapsis states (before and after the maneuver) are formed. The states are propagated forward and backward in time from periapsis to the sphere-of-influence crossing. Luidens provides an analytical expression for the time of propagation.[14]

Broad search algorithm

For a given family, the repeat period is denoted T (integer multiple of T_{syn}), where $t_f - t_0 = T$. The algorithm is summarized as follows:

1. For a given initialization year, the Earth-Mars (or Mars-Earth) Hohmann transfer time t_0^* and flight time Δt_H are determined.

2. The set of initial (seed) legs which are near-Hohmann are constructed. This is done via Lambert solutions over a grid of departure epochs t_0 and flight times Δt_1. The grids are defined as:

$$t_0 \in \{t_0^{\min}, \ t_0^{\min} + \Delta t_0, \ \cdots, \ t_0^{\max}\} \qquad \text{where, } t_0^{\min} < t_0^* < t_0^{\max}$$
$$\Delta t_1 \in \{\Delta t_H^{\min}, \ \Delta t_H^{\min} + \Delta t_0, \ \cdots, \ \Delta t_H^{\max}\}$$
$$\Delta t_H^{\min} = \Delta t_H + t_0^{\min} - t_0^* \qquad \Delta t_H^{\max} = \Delta t_H + t_0^{\max} - t_0^*$$

3. For each seed leg:

    (a) The set of feasible leg 2 options are computed over a grid of Δt_2, and for all possible revolutions (and fast/slow arcs).

    (b) The set of feasible final leg options are determined over a grid of Δt_f values (t_f is known).

    (c) For six total flybys, options for the third leg are determined similarly.

    (d) For each feasible combination of legs, the last remaining (un-computed) leg is assessed for feasibility.[‡]

   (e) All fully feasible solutions are saved.

[‡]There is only one flight time, but the number of revolutions and fast/slow arc are still enumerated.

Figure 3 illustrates how an EMEVVE broad search progresses from a single seed, and the multiple arrows indicate a grid search over flight times (as opposed to a single flight time). For the results that follow $t_0^{\min}$ and $t_0^{\max}$ are selected so that the initial (seed) leg epochs t_0 and flight times Δt_1 do not deviate more than 50-days from that of the Hohmann transfer. The set of seed legs are also filtered to ensure that the excess speed at Earth/Mars are below a maximum $v_\infty^{\max} = 5$ km/sec. For all other legs, flybys must be evaluated to check constraints on v_∞ matching and altitude. For an interior flyby at time t_i, the following constraints are applied to determine feasibility:

$$\|v_\infty(t_i^+) - v_\infty(t_i^-)\| < \Delta v_\infty^{\max} \qquad 100 \text{ km} < r_p(t_i) - R_{\text{planet}} < 100,000 \text{ km} \qquad (7)$$

And $v_\infty^{\max}$ is selected to be between 100 and 200 m/sec. A final step ensures there are no unintended intermediate flybys along the trajectory. This is applied as a final filter upon the completion of a search.
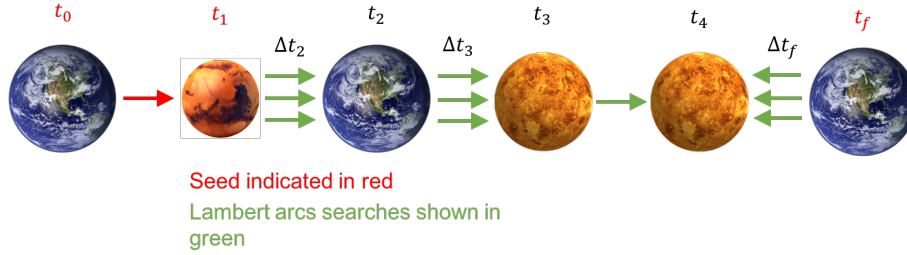
Figure 3: Broad Search Diagram for the EMEVVE Family from a Single Seed

Multi-cycle trajectories

The algorithmic procedure is repeated for each combination of itinerary family and Earth-Mars (or Mars-Earth) epoch of opportunity. Because the planetary alignment is not exactly repeatable, the results are not necessarily feasible when propagated past the first cycle. To ensure repeatability while maintaining the desired low-energy characteristics, a routine is developed to match sets of single cycle trajectories. For example, a set of one synodic period solutions starting in 2020 may be matched with another set of one synodic period solutions starting in 2026. The combinatorial matching is far less computationally expensive than performing a broad search (involving Lambert evaluations) over two or more cycles (more than 10 to 12 encounters). The matching also permits the mixing of cycler families (e.g. an EMEEVE followed by a EMEVVE) which may be advantageous at times. Often, however, a simple shift in the middle (interior leg) flight times within a given family is sufficient to maintain feasibility into the next cycle.

Optimizing in the true ephemeris

High quality approximate solutions (single or multi cycle) are those with low excess speed and low Δv costs. Flyby altitudes are considered as a secondary valuation criterion. The final aspect of the methodology involves optimizing select high-quality solutions to be continuous and ballistic using high-fidelity dynamics. A two-step continuation (homotopy) is used. Step 1 includes the gravity of the Sun and the planets and is iterated to achieve continuity. This converged solution is used as the initial guess to the second step which adds the gravity of all planets and the Earth's moon. The following are enforced on the optimization:

1. Periapsis altitudes between 100 km and 100,000 km for all flybys.

2. Trajectory continuity to a tolerance of 1.0E-3 km in position and 1.0E-6 km/sec in velocity.

A control-point (CP) break-point (BP) model is used, where integration occurs forward and backward from each control point, and continuity is enforced at the break-points (points between adjacent control points). The initial state at each control point is taken from a resulting broad search solution, and the hyperbolic flyby orbits take precedence (over the Sun-centered Lambert arcs). SNOPT is used as the underlying SQP optimizer. [15] Much effort is taken to set bounds, scaling, and step-size control for the state and time parameters to ensure quality convergence.

BROAD SEARCH RESULTS

No feasible solutions were found (of any family) with a repeat period of one synodic period (6.4 years). However, there were trajectories involving a single subsurface flyby, that were otherwise feasible. It is possible, albeit unverified, that reasonably small deep-space maneuvers could enable one synodic period triple cyclers that do not go subsurface. In contrast, thousands of feasible two-synodic period cyclers were obtained. Itineraries with six flybys and consecutive Earth or Venus encounters (e.g. EMEVVE and EMEEVE) seemed to exhibit the best overall characteristics. Figures 4-5 illustrate example cycler trajectories projected on the ecliptic plane and propagated over the first cycle.
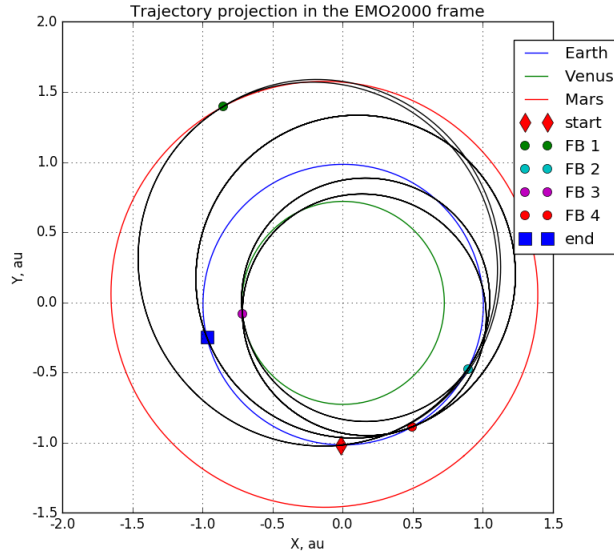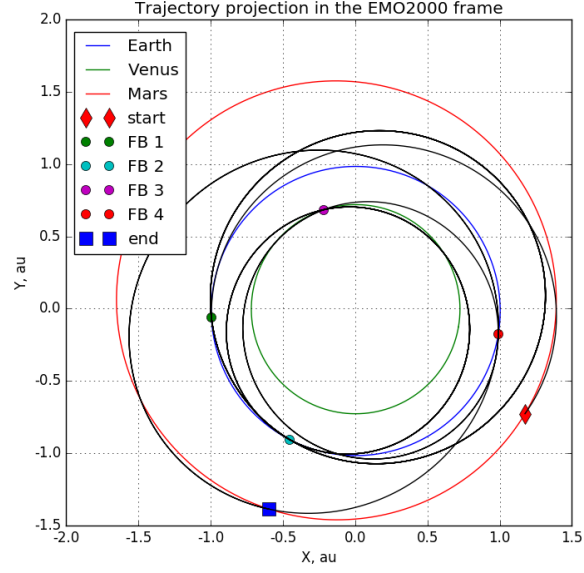

Figure 4: Ecliptic projection of example *outbound* EMEVEE family cycler starting in 2020

The matching algorithm was successfully used to construct trajectories covering two cycles (25.6 years of total flight time), with average transit leg v_∞ below 5 km/sec. The excess speed is very important since it is proportional to the amount of fuel any taxi vehicle would need to expend. For comparison, one of the best Earth-Mars cyclers (the S1L1) has maximum excess speed exceeding 7 km/sec. [2]

Figure 6 depicts an example EMEVVE cycler that begins in 2022 and ends after two cycles. Recall that the repeat period T is 12.8 years. Table 2 summarizes the encounter dates and energy

Figure 5: Ecliptic projection of example *inbound* MEEVEM family cycler starting in 2022
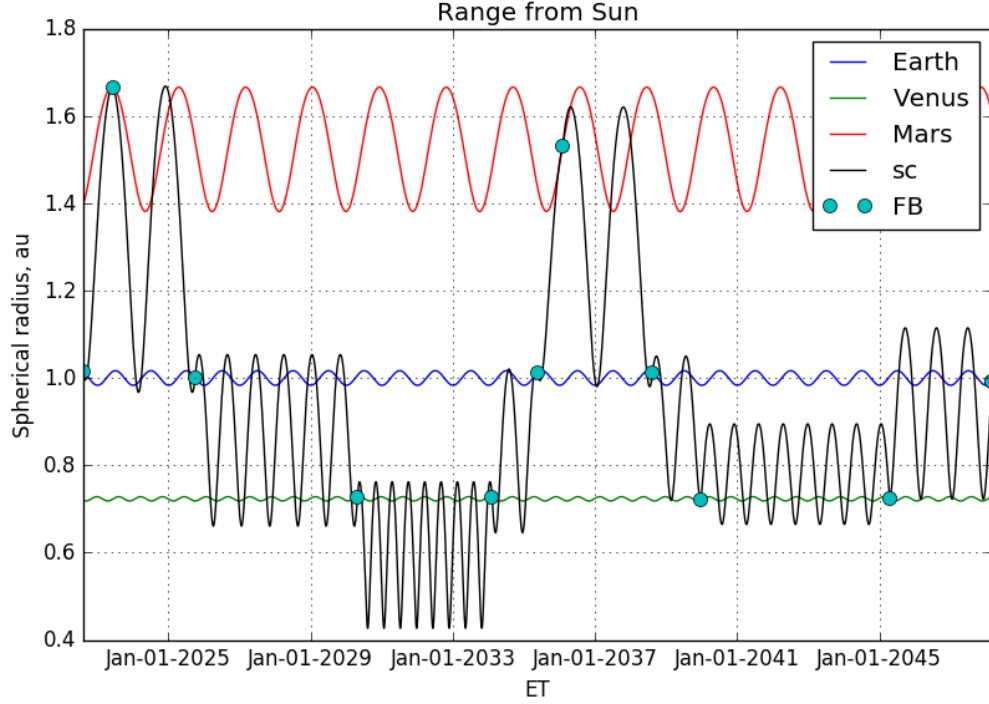
Figure 6: EMEVVE family cycler (outbound) starting in 2022, for two repeat periods

characteristics for this *outbound* trajectory. The transit leg flight times are 309 and 259 days. Shorter transit times are possible but most often this comes with higher v_∞. In Table 3 an MEEVEM *inbound* cycler is outlined, also with start epoch in 2022. Here the transit leg flight times are 268 and 223 days.

9

Table 2: Flyby summary for EMEVVE family cycler over two repeat periods

Flyby body	Date	Excess speed, km/sec	Periapsis altitude, km	Flight Time, days
Earth	07-Aug-2022	4.72	100	-
Mars	12-Jun-2023	2.50	4,164	309
Earth	01-Oct-2025	5.81	3,814	842
Venus	26-Apr-2030	7.00	684	1668
Venus	08-Feb-2034	7.00	1,985	1384
Earth	22-May-2035	4.21	1,998	468
Mars	05-Feb-2036	2.79	1,754	259
Earth	15-Aug-2038	5.04	3,213	922
Venus	26-Dec-2039	4.49	3,319	498
Venus	17-Apr-2045	4.49	836	1939
Earth	05-Mar-2048	5.67	100	1053

Table 3: Flyby summary for MEEVEM family cycler over two repeat periods

Flyby body	Date	Excess speed, km/sec	Periapsis altitude, km	Flight Time, days
Mars	24-Jun-2022	3.85	100	-
Earth	19-Mar-2023	3.48	7,831	268
Earth	28-Aug-2024	3.42	967	528
Venus	13-Mar-2028	5.16	29,777	1293
Earth	02-Oct-2032	3.84	2,545	1664
Mars	08-Apr-2035	3.12	249	918
Earth	17-Nov-2035	2.98	3,719	223
Earth	23-Apr-2039	2.92	2,224	1253
Venus	23-Oct-2039	4.31	12,349	183
Earth	11-Aug-2045	4.97	7,484	2119
Mars	21-Jan-2048	2.42	100	893

OPTIMIZED RESULTS

Some high-quality cases (*inbound* and *outbound*) from the broad search were optimized, and most could be made to be ballistic under realistic gravitational dynamics. Table 4 outlines an example optimal *inbound* and *outbound* pair of cycler trajectories starting in 2020, with taxi vehicle Δv computed assuming a 100 km altitude parking orbit at Earth and Mars. Transporting at every opportunity would require a total of twelve cycling transport vehicles (6 *inbound* and 6 *outbound*). A total of seven round-trip crewed missions may be extracted and analyzed from Table 4. For example, a crew would launch from Earth in late-June 2020 and expend 4.22 km/sec of Δv to rendezvous with a transport vehicle already on the cycler. After a 309-day transit, the crew use 2.24 km/sec of taxi vehicle Δv to capture at Mars, where they will remain until June 2022 (415-day stay). The crew will then expend 2.77 km/sec to rendezvous with an *inbound* transport, returning them to Earth in 268-days. The 992-day mission will complete with a 3.78 km/sec capture burn at Earth.

For this architecture, transit leg flight times vary from 219 to 309 days, and the taxi vehicle Δv is between 2.04 and 4.28 km/sec. By comparison, one of the best S1L1 Earth-Mars cyclers in Ref. [2] has flight times between 115 to 223 days, but the taxi vehicle Δv can be up to 5.33 km/sec at Earth and 5.64 km/sec at Mars. Over many missions, the fuel/mass penalty associated with higher Δv to rendezvous could be significant. Of course, the added efficiency comes with generally longer flight times and the need for twelve transport vehicles to cover every Earth-Mars and Mars-Earth opportunity (compared with four for the S1L1, and two for the Aldrin cycler).

Table 4: Example transit characteristics for triple cycler transportation architecture

	Outbound					Inbound			
Body	Date	v_∞, km/sec	Transit, days	Taxi Δv, km/sec	Body	Date	v_∞, km/sec	Transit, days	Taxi Δv, km/sec
Earth	30-Jun-2020	4.76		4.22	Mars	24-Jun-2022	3.85		2.77
Mars	05-May-2021	2.90	309	2.24	Earth	19-Mar-2023	3.48	268	3.78
Earth	26-Sep-2022	4.88		4.28	Mars	25-Jul-2024	2.94		2.26
Mars	08-May-2023	2.59	224	2.09	Earth	15-May-2025	2.95	294	3.64
Earth	28-Sep-2024	3.59		3.82	Mars	26-Aug-2026	3.16		2.37
Mars	03-Aug-2025	2.55	309	2.07	Earth	11-Jun-2027	3.47	289	3.78
Earth	05-Oct-2026	3.70		3.85	Mars	05-Oct-2028	2.79		2.18
Mars	05-Aug-2027	2.99	304	2.29	Earth	10-Aug-2029	4.71	309	4.21
Earth	02-Jan-2029	4.20		4.02	Mars	03-Dec-2030	2.73		2.15
Mars	03-Sep-2029	3.76	244	2.72	Earth	25-Jul-2031	4.61	234	4.17
Earth	21-Dec-2030	3.58		3.81	Mars	14-Feb-2033	2.48		2.04
Mars	11-Sep-2031	3.66	264	2.66	Earth	21-Sep-2033	3.41	219	3.76
Earth	14-Apr-2033	4.26		4.04	Mars	08-Apr-2035	3.12		2.35
Mars	04-Dec-2033	3.93	234	2.82	Earth	17-Nov-2035	2.97	223	3.64

CONCLUSIONS

Trajectories which ballistically cycle between Venus, Earth, and Mars are presented and analyzed for the first time. Thousands of previously undocumented triple cyclers have been discovered. The addition of Venus to the previously studied Earth-Mars cycler architecture can yield improved energy characteristics for transit legs. Triple cyclers may be considered an alternative system for enabling mass transport between Earth and Mars, particularly for maximizing payload mass while accepting somewhat longer flight times and the need for more transport vehicles. Lastly, the triple cycler concept is extensible to other systems which have near-commensurate periods, such as Io-Europa-Ganymede in the Jovian system.

ACKNOWLEDGMENTS

REFERENCES

[1] D. V. Byrnes, J. Longuski, and B. Aldrin, "Cycler Orbit Between Earth and Mars," *Journal of Spacecraft and Rockets*, Vol. 30, No. 3, 1993, pp. 334–336.

[2] T. T. McConaghy, D. F. Landau, C. H. Yam, and J. M. Longuski, "Notable Two-Synodic-Period Earth-Mars Cycler," *Journal of Spacecraft and Rockets*, Vol. 43, No. 2, 2006, pp. 456–465, 10.2514/1.15215.

[3] R. P. Russell and C. Ocampo, "Systematic Method for Constructing Earth-Mars Cyclers Using Free-Return Trajectories," *Journal of Guidance, Control, and Dynamics*, Vol. 27, No. 3, 2004, pp. 321–335, 10.2514/1.1011.

[4] D. M. Pisarevsky, A. Kogan, and M. Guelman, "Interplanetary Periodic Trajectories in Two-Planet Systems," *Journal of Guidance, Control, and Dynamics*, Vol. 31, No. 3, 2008, pp. 729–739, 10.2514/1.30046.

[5] D. F. Landau and J. M. Longuski, "Mars Exploration via Earth-Mars Semi-Cyclers," *AAS Paper 05-269*, 2005.

[6] R. Moir and W. Barr, "Analysis of interstellar spacecraft cycling between the Sun and the near stars," *Journal of the British Interplanetary Society*, Vol. 58, 2005, pp. 332–341.

[7] A. E. Lynam and J. M. Longuski, "Laplace-resonant triple-cyclers for missions to Jupiter," *Acta Astronautica*, Vol. 69, No. 3-4, 2011, pp. 158–167, 10.1016/j.actaastro.2011.03.011.

[8] S. Hernandez, D. Jones, and M. Jesick, "Families of Io-Europa-Ganymede Triple Cycler," to appear in proceedings of the 2017 AAS/AIAA Astrodynamics Specialists Conference, 2017.

[9] A. Vanderveen, "Triple-planet ballistic flybys of Mars and Venus.," *Journal of Spacecraft and Rockets*, Vol. 6, No. 4, 1969, pp. 383–389, 10.2514/3.29667.

[10] M. Okutsu and J. M. Longuski, "Mars Free Returns via Gravity Assist from Venus," *Journal of Spacecraft and Rockets*, Vol. 39, No. 1, 2002, pp. 31–36, 10.2514/2.3778.

[11] N. Strange and J. M. Longuski, "Graphical Method for Gravity-Assist Trajectory Design," *Journal of Spacecraft and Rockets*, Vol. 39, No. 1, 2002, pp. 9–16.

[12] R. P. Russell, *Global Search and Optimization for Free-Return Earth-Mars Cyclers*. PhD thesis, The University of Texas at Austin, 2004.

[13] J. Englander, B. Conway, and T. Williams, "Automated Mission Planning via Evolutionary Algorithms," *Journal of Guidance, Control, and Dynamics*, Vol. 35, No. 6, 2012, pp. 1878–1887, 10.2514/1.54101.

[14] R. Luidens, B. Miller, and J. Kappraff, "Jupiter High-Thrust Round-Trip Trajectories," tech. rep., NASA, 1966.

[15] P. E. Gill, W. Murray, and M. A. Saunders, "SNOPT: An SQP Algorithm for Large-Scale Constrained Optimization," *SIAM Journal on Optimization*, Vol. 12, No. 4, 2002, pp. 979–1006, 10.1137/S1052623499350013.